HHS Public Access

Author manuscript

Thromb Haemost. Author manuscript; available in PMC 2018 March 12.

Published in final edited form as:

Thromb Haemost. 2016 August 30; 116(3): 506–516. doi:10.1160/TH15-11-0848.

Leukemia-associated Rho guanine nucleotide exchange factor (LARG) plays an agonist specific role in platelet function through RhoA activation

Siying Zou[1], **Alexandra M. Teixeira**[2], **Mingzhu Yin**[2,3], **Yaozu Xiang**[4,5], **Juliana Xavier-Ferruccio**[4,6], **Ping-xia Zhang**[4,6], **John Hwa**[4,5], **Wang Min**[2,4], and **Diane S. Krause**[1,2,3,4,6]

[1]Department of Cell Biology, New Haven, CT, USA

[2]Pathology, New Haven, CT, USA

[3]Interdepartmental Program in Vascular Biology and Therapeutics, New Haven, CT, USA

[4]Department of Laboratory Medicine, New Haven, CT, USA

[5]Division of Cardiovascular Medicine, Department of Internal Medicine, New Haven, CT, USA

[6]Yale Stem Cell Center; Yale School of Medicine, New Haven, CT, USA

Summary

Leukemia-**A**ssociated **R**ho**G**EF (LARG) is highly expressed in platelets, which are essential for maintaining normal hemostasis. We studied the function of LARG in murine and human megakaryocytes and platelets with *Larg* knockout, shRNA-mediated knockdown and small molecule-mediated inhibition. We found that LARG is important for human, but not murine, megakaryocyte maturation. *Larg* KO mice exhibit macrothrombocytopenia, internal bleeding in the ovaries and prolonged bleeding times. KO platelets have impaired aggregation, α-granule release and integrin α2bβ3 activation in response to thrombin and thromboxane, but not to ADP. The same agonist-specific reductions in platelet aggregation occur in human platelets treated with a LARG inhibitor. *Larg* KO platelets have reduced RhoA activation and myosin light chain phosphorylation, suggesting that Larg plays an agonist-specific role in platelet signal transduction. Using 2 different in vivo assays, *Larg* KO mice are protected from *in vivo* thrombus formation. Together, these results establish that LARG regulates human megakaryocyte maturation, and is critical for platelet function in both humans and mice.

Corresponding Author: Diane S. Krause, diane.krause@yale.edu, Tel: 203-785-7089, Fax: 203-785-4305, Address: Yale Stem Cell Center, 10 Amistad Street, Room 214I New Haven, CT 06509.

Authorship Contributions: S.Z. performed experiments, analyzed data, and wrote the manuscript; A.M.T., M.Y., J.X-F. and Y.X. performed experiments, analyzed data and contributed to the manuscript; P.Z. provided technical support and performed experiments. W.M. and J.H. oversaw experiments, and provided intellectual input. D.S.K. oversaw the project, provided intellectual input and wrote the manuscript.

Disclosure of Conflicts of Interest: The authors declare no competing financial interests.

Introduction

Hemostasis and pathological thrombus formation are dynamic processes involving a coordinated series of platelet activation events, which require bidirectional cellular signaling leading to granule secretion (1). Platelet agonists such as Adenosine Diphosphate (ADP), thrombin and thromboxane activate platelets via agonist-specific membrane-bound G protein coupled receptors (GPCR), which transduce signals via small Gα subunits to activate downstream effectors including the Rho GTPases (1). There are four families of Gα subunit, Gα12/13, Gαq, Gαi and Gαs (2, 3). Previous studies have established which Gα subunits are associated with the major platelet agonist receptors.[4, 5] However, there are gaps in our knowledge regarding how signals are transduced from the Gα subunits at the membrane to activate Rho GTPases within platelets. Guanine exchange factors (GEF) are known to couple Gα subunits and Rho signaling (6), and there are multiple GEFs expressed in platelets that can potentially function in platelet signal transduction from Gα subunits to RhoA. Here, we test the hypothesis that **L**eukemia **A**ssociated **R**ho**G**EF (LARG) plays a critical role in platelet signal transduction.

LARG was first identified as part of a MLL (Mixed Lineage Leukemia) - LARG fusion protein found in an acute myeloid leukemia patient (7). Publically available expression data on human platelets reveals that LARG is the most highly expressed guanine exchange factor in platelets (top 4%) (8). A previous study showed that LARG KO mice on the C57B6 background are embryonic lethal, however homozygous KO mice on the mixed CD1 and C57B6 background are viable with no obvious developmental defects (9). When all three RGS RhoGEF family members (LARG, p115-RhoGEF and PDZ-RhoGEF) are deleted from murine embryonic fibroblasts, thrombin signaling is abolished (9). Because thrombin is a critical platelet activator (10), we hypothesized that LARG deficiency or inhibition would affect thrombin-induced platelet activation by decreasing thrombin-induced RhoA activation.

We assessed the role of LARG in platelet function by characterizing the *in vitro* and *in vivo* megakaryocyte and platelet phenotypes of *Larg* KO mice, and by assessing human megakaryocyte (MK) and platelet function in the presence of a LARG inhibitor. Murine MK were assessed in *Larg* KO mice and human megakaryopoiesis was assessed in vitro using shRNA and inhibitor treatments. We found that LARG is important for human MK maturation, but *Larg* KO mice had no detectable differences in megakaryopoiesis. However, LARG appears to play a role in activation of both murine and human platelets specifically in response to thrombin and thromboxane via activation of RhoA signaling. Moreover, LARG was shown to play an important role in two *in vivo* murine thrombosis models, carotid artery ligation and $FeCl_3$ induced carotid damage.

Materials and Methods

Mice

LARG KO mice.on a mixed CD1 and C57B6 background (9) were generously provided by the Gutkind laboratory (NIDCR, NIH), and all studies were performed with WT littermate

controls to eliminate potential interference from strain background. Procedures were approved by the Yale University Institutional Animal Care and Use Committee (IACUC).

Western Blot

Murine washed platelets were directly lysed in Laemmli sample buffer (Bio-Rad) containing β-mercaptoethanol. Lysates were resolved on Bio-Rad precast gradient gels (4-20%) and transferred to nitrocellulose membranes. After blocking (5% non-fat dried milk in Tris buffered saline (TBS) with 0.1% Tween-20), membranes were probed with anti-LARG (1:200; Santa Cruz),or anti-GAPDH (1:5000; Sigma) antibody overnight at 4 °C. For phosphorylated MLC detection, platelet blots were incubated with anti-phosphorylated MLC (1:1000, Cell Signaling) overnight at 4 °C. Blots were quantified using GeneTools Imaging software from Syngene.

RNA analysis

Total RNA from washed platelets was extracted using the RNAqueous-Micro Kit (Millipore) and cDNA synthesized with Iscript cDNA Synthesis Kit (BioRad). Applied Biosystems (Life Technologies) Taqman Gene Expression Assays were used for quantification on a CFX96 C1000 thermal cycler (Bio-Rad, California). Taqman Probes were as follows: Itga2b (Mm00439741_m1); Actn1 (Mm01304398_m1); p115-RhoGEF (Mm00476230_m1); GEF-H1 (Mm9943757_m1); LARG (Mm00804308_m1).

Determination of bleeding time

Using a sharp razor blade, 0.5 cm of the tail of 4-week old anesthetised (30% Isoflurane, Henry Schein Animal Health) WT versus KO littermate was transected and the tail was held in warm PBS. Time until cessation of tail bleeding was measured. Persistent bleeding was terminated after 5 minutes.

Plasmids, Virus Production, and Primary MK Progenitor Transduction

LARG lenti-viral shRNA (human) set (TRCN0000298870, 298841, 298842) and non-target shRNA control (SHC002) and (murine) set (TRCN0000109960; TRCN0000109963) and non-target shRNA control (SHC002) were purchased from Sigma (St. Louis, MO, USA). For lenti-virus production, control vector or LARG shRNA, gag-pol and VSVG packaging plasmids were transfected into 90% confluent HEK293 cells with FuGene6 (Promega, Madison, WI, USA) using manufacturer's instructions. Supernatant collected at 48, 72 and 96 hr post transfection was combined, spun at 3,700 × g through MW 100 kDa Amicon filters (Millipore, Billerica, MA, USA) to concentrate the virus to approximately $1\text{-}3\times10^8$ ifu/ml, and aliquots were stored at −80°C.

Two different subpopulations of human G-CSF mobilized peripheral blood cells were used. MEPs were isolated as Lin-CD34+CD45RA-Flt3-CD110+CD36- by FACS Aria (BD Biosciences, San Jose, CA, USA), and lineage negative cells were isolated by immunomagnetic depletion (EasySep™ Human Progenitor Enrichment Kit with Platelet Depletion, Stem Cell Technologies). Freshly sorted human MEP cells in human expansion medium (StemSpan medium (StemCell Technology, Vancouver, Canada) with 30% BIT, 20ng/ml human thrombopoietin, and 10 ng/ml IL3 (all cytokines from ConnStem, Cheshire,

CT)) were infected with indicated viruses in the presence of polybrene (8 mg/ml, Sigma, St. Louis, MO, USA) by spinfection at 900g for 1.5 hr at 30°C. After 4 days in expansion medium, cells were switched to differentiation medium (CC220 cytokine mixture (StemCell Technology, Vancouver, Canada) with StemSpan and 30% BIT) together with 1ug/ml puromycin (Sigma, St. Louis, MO, USA) selection for another 6 days. Knockdown efficiency was confirmed by qRT-PCR. Murine PreMegE (11) cells (Lin-Sca-Kit+CD41-CD105-CD150+) were sorted from fresh bone marrow and expanded in StemSpan supplemented with 30% BIT9500, 100 ng/ml murine SCF, 50 ng/ml murine Flt3-L, 10 ng/ml murine IL-3, 50 ng/ml murine TPO. 24 hour post expansion, cells were infected with indicated viruses in the presence of polybrene (8 mg/ml, Sigma, St. Louis, MO, USA) by spinfection at 900g for 1.5 hr at 30°C. For murine MK differentiation, after 2 days in expansion medium, cells were switched to differentiation medium with 20 ng/ml of murine TPO, together with 1ug/ml puromycin (Sigma, St. Louis, MO, USA) and selected for another 3 days. DNA ploidy and MK surface markers were analyzed by flow cytometry.

Flow Cytometric Analysis of MK DNA Content and Surface Markers

For ploidy assay, fresh bone marrow cells or *in vitro* differentiated MKs were stained with FITC-conjugated anti-CD41 antibody, then fixed and permeabilized using 70% ethanol at 4°C overnight. After incubation with 4 μg/ml RNAase at 37°C for 4 hrs, 10 μg/ml propidium iodide (Sigma, St. Louis, MO, USA) was added and cells analyzed using a FACS Calibur cytometer (BD Biosciences, San Jose, CA, USA). For cell surface marker analysis, fresh bone marrow cells or in vitro differentiated MKs were stained with APC-conjugated anti-CD41, PE-conjugated anti-CD42 antibody and DAPI (1:1000). Cells were analyzed with an 8-Color Stratedigm Cytometer (San Jose, CA, USA). Flow cytometric data were analyzed with FlowJo software (TreeStar, Ashland, OR, USA).

Murine Platelet Preparation

Blood was collected into tubes containing 3.2% sodium citrate (Medicago, Sweden). Platelet-rich plasma (PRP) was obtained by centrifugation of whole blood at 200g for 8 min. For washed platelets, an additional 1/10 volume of 3.2% sodium citrate was added to the blood with 1ml of Aggregation Wash Buffer (0.5mM MgCl2, 10mM HEPES, 140mM NaCl, 3mM KCl, 5.5mM Glucose, 0.5mM NaH2PO4, 5mM NaHCO3, 0.3% BSA), and the platelets were recovered after centrifugation at 190g for 10 min. Platelets were then pelleted at 4000g, 2 min, and resuspended at 1×10^8 - 2×10^8/ml in Aggregation Wash Buffer with apyrase (0.02U/ml, New England Biolabs). Platelets were incubated at 37°C for 30min before aggregation experiments. For platelet counts and volume, blood was collected from the retro-orbital sinus using EDTA coated tubes, and assessed using a Hemavet 950FS analyzer (Drew Scientific).

Human Platelet Preparation

Human blood was collected under an IRB approved protocol. Venous blood was drawn from healthy volunteers into 1/10 volume 3.2% Sodium Citrate. PRP was obtained by centrifugation at 250g at 25°C for 15 min, and the platelet count in the PRP determined using Hemavet 950FS analyzer (Drew Scientific). Platelet-poor plasma (PPP) was obtained by centrifugation of remaining blood at 1400g at 25°C for 10 min. The PRP was adjusted

with PPP to 2–3 × 10^8 platelets/ml suspension. For washed platelets, platelets from PRP were pelleted (1000g, 15 min) and resuspended in wash buffer (103 mM NaCl, 5 mM KCl, 1 mM MgCl2, 5 mM glucose, 36 mM citric acid, pH 6.5) containing 3.5 mg/ml BSA (Sigma-Aldrich). After sedimentation, the platelets were washed twice in wash buffer and resuspended at 2–3 × 10^8 platelets/ml in buffer composed of 5 mM HEPES, 137 mM NaCl, 2 mM KCl, 1 mM MgCl2, 12 mM NaHCO3, 0.3 mM NaH2PO4, and 5.5 mM glucose, pH 7.4, containing 3.5 mg/ml BSA.

Platelet Aggregometry

Mouse and human platelet (2×10^8 platelets/ml) aggregation was performed with washed platelets using a Chrono-log Model 700 Whole Blood/Optical Lumi-Aggregometer with AGGRO/LINK software (Chrono-log), stirring at 1200 rpm at 37°C. Adenosine diphosphate (ADP) induced aggregation was performed in the presence of human fibrinogen (0.5mg/ml, Sigma-Aldrich). Agonists were used at concentrations indicated: ADP (Chrono-log), Collagen (Chrono-log), thrombin (Roche), U46619 (Cayman Chemical Company).

Murine platelet assessment by flow cytometry

50 uL of whole blood was collected via the retro-orbital sinus into heparinized tubes (BD Biosciences, San Jose, CA) and was washed three times in Tyrodes-HEPES and then resuspended in Tyrodes-HEPES with 2mM CaCl2. Platelets were stimulated for 15 min at 37°C with indicated concentrations of ADP, U46619, or thrombin, and activation was assessed with FITC CD41/61 (αIIbβ3), phycoerythrin (PE)-labeled anti-JON/A, and PE labeled anti-P-selectin/CD62P (Emfret Analytics, Germany). Activation was terminated by adding 5×volume 0.5% paraformaldehyde. Data was collected on a FACSCalibur (BD Biosciences) and analyzed using FlowJo software (Tree Star).

For reticulated platelets, whole blood was stained with 0.1μg/ml thiazole orange (Sigma-Aldrich) for flow cytometric analysis. Platelet populations were identified by FSC/SSC gate and reticulated platelet percentage was calculated as the ratio of thiazole orange positive platelets/total platelets.

RhoA G-LISA Activation Assay

Washed platelets were isolated and stimulated with indicated agonists for 1min, then placed on dry ice to stop reaction. Lysis buffer was added and lysate was cleared by centrifugation at 14,000g for 5 minutes at 4-6°C. Lysate from unstimulated platelets were used as baseline control and GTPase activity was assayed according to RhoA G-LISA activation Assay Kit protocols (Cytoskeleton) and luminescent signal was read with Envision 2104 Multilabel Reader (PerkinElmer).

Platelet Immunofluorescence

Resting platelets (5×10^3/ul) were centrifuged onto poly-L-lysine coated coverslips (Warner Instruments), and fixed in 4% paraformaldehyde. To analyze spread platelets, platelets were stimulated with 0.01U/ml thrombin and allowed to spread on glass coverslips for 30 min at room temperature prior to paraformaldehyde fixation. Platelets were then permeabilized (0.1% Triton X-100 in PBS) and blocked (2% FBS/2% BSA in PBS) overnight. Coverslips

were incubated with anti-β-tubulin (1:250; Sigma-Aldrich) for 2 hours at room temperature, followed by incubation with secondary antibody (1:500 Goat-anti-mouse-488, Invitrogen) and stained with Phalloidin (1:200, Life Technologies). After washing, coverslips were mounted with Aqua Poly/Mount (Polysciences, Inc.). Images were captured using a Leica SP5 confocal microscope (Leica Microsystems, Germany).

Carotid Artery Ligation

The carotid artery ligation model was performed as described (12). Briefly, the left common carotid artery was ligated near the carotid bifurcation. After 14 days, mice were euthanized. The left and right arteries were photographed, fixed in 4% paraformaldehyde, embedded in OCT compound, and sectioned for analysis. 100 contiguous sections were obtained per mouse: 60 of these sections were used for H&E staining and quantification, and the other 30 sections were used for immunofluorescence with anti-mouse CD41-FITC (Biolegend) and quantification. Thrombus formation assessed on H&E stained sections was quantified as percentage of occluded area versus total area of the section as previously reported (13).

Ferric Chloride Injury Model

Experiments were performed as previously described (14). Briefly, 10 to12-week-old littermate mice were anesthetized by intraperitoneal injection of ketamine (100mg/kg; Ketaset, Fort Dodge Animal Health). The right carotid artery was dissected and a patch of Whatman filter paper (1×2 mm^2) soaked with 10% ferric chloride ($FeCl_3$) was applied to the ventral surface of the carotid artery for 2 minutes. The patch was removed and artery surface was flushed with saline. To determine the time to occlusion, a Doppler flowprobe (Model 0.5 PSB; Transonic Systems) was placed at the surface of the carotid artery and blood flow was recorded using a Transonic Model TS420 flowmeter (Transonic Systems) up to 20 min.

Statistical Analysis

Statistical significance was assessed set at $P<0.05$ and using Prism 6.0 software (GraphPad Software) using the standard t-test statistical analysis.

Results

LARG deficiency results in prolonged bleeding time with internal bleeding

Western blot analysis confirmed Larg expression in WT murine platelets as well as the complete loss of Larg protein in *Larg* KO platelets (Fig 1A). Complete blood counts showed that KO mice have small, but statistically significant decrease in platelet count ($P<0.01$) and increase in platelet size ($P<0.005$, Fig.1B-C). Flow cytometry on whole blood with thiazole orange staining showed that *Larg* KO mice also have a higher percentage of reticulated platelets (Fig S1). Necropsy revealed hemorrhagic lesions in the ovaries of KO mice (Fig 1D), with no obvious defects observed in other major organs (lung, heart, kidney, spleen, liver) (Fig S2). H&E staining of ovarian sections revealed hemorrhage with normal oocyte numbers (Fig S3) in *Larg* KO mice. Therefore, we postulated that *Larg* KO have bleeding defects resulting in hemorrhage. Consistent with this hypothesis, *Larg* KO mice have a

significantly prolonged bleeding time (Fig 1E) suggesting a significant role in platelet function and maintenance of normal haemostasis.

LARG may be essential for human MK but dispensable for murine MK maturation

To test the function of LARG in MK differentiation, we used lentiviral shRNA to knockdown *LARG* in primary human cells as they differentiated *in vitro* down the MK lineage. The shRNA vectors used also encode for puromycin resistance and puromycin was added to the medium on days 5-11 of culture. Results showed that *LARG* knockdown blocked MK maturation (CD41/CD42%) (Fig 2A-B). We used 3 different shRNAs to target different genomic regions of LARG. Each of the three shRNAs blocked MK differentiation to some degree, and the extent of inhibition of MK maturation correlated with the degree of LARG knockdown by the different shRNAs (Fig S4A-C). Analysis of cytospins of the puromycin selected cells revealed a lack of mature, polyploid MK in the *LARG* KD group compared to control shRNA (Fig S4D), consistent with a role in human MK maturation.

We studied LARG's role in the murine system by characterizing the MK phenotype in *Larg* KO mice. Flow cytometric analysis of bone marrow MK showed no significant difference in the percentage of CD41+ or CD41+CD42+ cells, nor any differences in ploidy of KO versus WT (Fig 2C) Mk. Moreover, there are no differences in MK maturation or polyploidization of KO bone marrow cells differentiated *in vitro* down the MK lineage (Fig 2D), suggesting that LARG is dispensable for murine MK differentiation. To rule out the effect of mouse strain background and to further assess the role of LARG in murine MK maturation, we used shRNA against murine LARG in *in vitro* WT MK differentiation culture. Consistent with the lack of differences between WT and KO Mk, with two different murine *Larg* shRNAs tested, no MK maturation defect was seen, suggesting that LARG does not play an important role in murine MK maturation (Fig S5).

LARG is critical for platelet function in response to thromboxane and thrombin in both mice and humans

To elucidate the function of LARG in platelets, aggregometry was performed with washed platelets from LARG KO versus WT littermate mice. Stimulation with low dose thrombin (0.004U) or the thromboxane analog U46619 (0.04 μM and 1 μM) led to pronounced aggregation of WT, but this was statistically significantly reduced in LARG KO platelets (Fig 3Ai-ii, S6A). This difference was masked with high dose thrombin (0.025U) (Fig 3Aiii). Previous studies have shown at low agonist concentrations, the thrombin receptor mediates platelet activation predominantly by coupling to Gα13, whereas higher agonist concentrations induce additional signaling via Gαq.(15, 16) This implies that LARG functions in response to thromboxane and thrombin through Gα13. Consistent with this specificity, there is no significant difference in the degree of platelet aggregation of KO vs WT platelet aggregation induced by ADP at either high (Fig 3A) or low doses, although we did observe a slight delay in platelet response at low doses of ADP (Fig 3Aiv, Fig S6B). In addition, when using collagen, in two out of three experiments we also observed a slight delay of platelet response to aggregate. However, like ADP, no difference in the maximum degree of aggregation was observed (Fig S6C). These data suggest that ADP and collagen

signaling may be slightly affected in LARG KO platelets, however, the more prominent and consistent defects of *Larg* deletion are in thrombin and thromboxane signaling.

To test whether the defective aggregation in KO platelets might be due to impaired inside-out integrin signaling, we used flow cytometry to assess for the conformational change of integrin αIIbβ3. Consistent with LARG playing a role in mediating the signal transduction induced by thromboxane, but not ADP, KO platelets showed significantly less integrin activation than WT in response to U46619, but not in response to ADP (Fig 4A). Also, no difference was seen in integrin activation in response to combined stimulation with ADP and U46619. Consistent effects of LARG deficiency were also observed when assessing for platelet α granule release by P-selectin exposure (Fig 4B). Whereas KO platelets exhibited defective α-granule release in response to low dose thrombin or PAR4-activating peptide (PAR4-AP), at higher agonist concentrations and combined stimulation of ADP together with U46619, no defects were observed (Fig 4B).

The results in mice cannot necessarily be extrapolated to human platelet activation due to species-specific differences in thrombin receptor (PAR) profiles (17). To assess the role of LARG in human platelets, aggregation assays were performed with freshly isolated human platelets in the presence of Y16, a LARG inhibitor developed by Dr. Yi Zheng's group (Cincinnati Children's Hospital), which inhibits LARG-mediated Rho activation in a dose-dependent manner (18). The control compound called ZINC has a similar chemical structure to Y16, but does not inhibit Rho activation. Consistent with the murine platelet data, Y16 preincubation inhibited platelet aggregation induced by very low dose thrombin (0.005U) (Fig 5A). Also, in response to higher concentrations of thrombin (0.1U) and thromboxane (U46619, 1uM), Y16 pretreated platelets aggregated to a lesser extent than in the DMSO and ZINC control groups (Fig 5B-C). The inhibition is dose-dependent (Fig S7A), and highly reproducible with multiple donors. However, Y16 did not affect aggregation induced by either ADP (Fig 5D, Fig S7B) or epinephrine (Fig S7C). Y16 is not 100% specific for LARG (18). We therefore assessed for differences in how Y16 affects integrin αIIbβ3 activation in response to thromboxane in WT versus *Larg* KO platelets (Fig S8). At a low dose (20 uM), Y16 causes a statistically significant decrease in WT platelets, but no significant difference in KO platelets. At higher doses (50 uM), while the inhibition in platelet activation was far greater for WT than KO platelets, there was a significant decrease in KO platelet activation as well, suggesting that other Y16 targets also regulate platelet function. Given the greater effect on WT platelets, the data are consistent with a role for LARG in murine and human platelet function. In addition, publically available data (8) from a healthy human cohort, show a potential positive correlation between LARG RNA levels and agonist response to PAR4-AP, while there is no correlation between LARG mRNA expression and response to ADP (data available on http://www.plateletomics.com/). Together, these data suggest that LARG does indeed play a pivotal role in platelet function, specifically in response to thromboxane and thrombin.

LARG KO platelets have compromised RhoA activation and myosin light chain (MLC) phosphorylation in response to thrombin and thromboxane stimulation

In order to gain insight into the mechanism by which LARG promotes platelet activation, we focused on Rho signaling. Specifically, the RhoA GLISA activation assay showed compromised RhoA activation in response to thrombin in LARG deficient platelets (Fig 6A). In addition, in contrast to previous published findings in the MK and platelet specific LARG KO (19), we did not observe differences in baseline RhoA activity in *Larg* KO platelets (Fig. 6A). We also assayed a downstream readout of RhoA signaling by assessing the phosphorylation of myosin light chain (MLC) in response to multiple agonists. Compared to WT littermate controls, KO platelets had a statistically significant decrease in MLC phosphorylation in response to thrombin and thromboxane, but showed no decrease in response to ADP stimulation (Fig 6B,C). We also tested whether activation of the PI3K-AKT pathway (20, 21) was affected in KO platelets by Western blot analysis for phosphorylated-AKT, but no obvious differences were observed between KO versus WT platelets (data not shown). Similarly, addition of the ROCK inhibitor Y27632 (10uM) to *Larg* KO platelets had no effect on platelet aggregation in response to 0.1U thrombin or 1uM U46619 (date not shown). These data suggest that there is defective Rho-ROCK-MLC signaling in LARG KO platelets in response to thrombin and thromboxane.

We tested whether there may be a compensatory increase in expression of related GEFs in the absence of LARG activity in platelets. We found there were no differences in the mRNA levels of p115-RhoGEF or GEF-H1 by RT-PCR (shown as Ct numbers) in LARG KO compared to WT platelets (Fig S9), suggesting that compensation by overexpression of these two GEFs in platelets does not occur in our KO model.

LARG is required for pathologic thrombus formation *in vivo*

Platelet inhibitory drugs are used clinically to prevent pathologic thrombus formation. To examine whether LARG plays a role in pathogenic thrombus formation *in vivo*, we compared thrombus formation between WT and LARG KO mice using two carotid artery injury models. In the carotid artery ligation model, 14 days post ligation, stable occlusion developed in 8 of 8 WT mice, but significantly less (in 2 of 8) or no (in 6 of 8) occlusion occurred in the KO mice (Fig 7A). Thrombus formation, quantified as percentage of occluded area versus total area of the section, was significantly decreased in the KO mice (Fig 7A-B). Platelet deposition, as determined by staining for CD41, was also significantly decreased in LARG KO mice (Fig 7C-D). In the ferric chloride injury model, thrombus development was monitored *in vivo* up to 20 min. While the majority of WT mice (7 of 8) formed a stable platelet clot in response to the chemical injury within 12 min, KO animals took significantly longer to form clots. Of 6 KO mice analyzed, 3 formed clots between 12 -5 minutes after injury, and the remaining 3 failed to form a clot at all (Fig 7E-F). Taken together, the data from these two *in vivo* thrombosis models provide evidence that LARG contributes to platelet thrombus formation *in vivo*, and suggest that, in theory, LARG inhibition could be used to decrease the risk of pathologic thrombi.

Discussion

We assessed the function of leukemia-associated RhoGEF (LARG) in primary murine and human megakaryocytes and platelets. Prior studies have investigated the role of LARG in smooth muscle cells and mouse embryonic fibroblasts (9, 22, 23). Consistent with a recent study reporting the effects of *Larg* KO in the megakaryocyte/platelet lineage (PF4-Cre promoter driven deletion) (19) in mice, we show that Larg plays a pivotal role in platelet signaling downstream of thrombin and thromboxane receptors, resulting in impaired haemostasis in response to trauma and marked protection from pathogenic arterial thrombus formation. Our studies go on to show potential roles of LARG in human megakaryocytes and platelets. In addition, in contrast to the study of Williams et al. (19), we show that Larg acts by activating RhoA.

The observation that LARG may be important for human but not murine MK maturation suggests differences in human and murine hematopoiesis. Although humans and mice are evolutionarily close, murine and human hematopoietic stem and progenitor cells have different phenotypic markers (24–27), and often the same protein (e.g. Hox B4) can have different effects on mouse and human stem and progenitor cells (28–30). These differences may signify functional differences in stem cell maintenance, differentiation, and microenvironmental interaction pathways between murine and human hematopoiesis (31), which may have important biological and translational implications (32).

Although dispensable for murine MK maturation, LARG is important for baseline hemostatic function in the absence of injury. The ovarian hemorrhages observed in LARG KO mice are reminiscent of hemorrhagic corpus luteum or hemorrhagic ovarian cysts that are sometimes observed in women with Von Willebrand Disease (33). In addition, cases of corpus luteum hemorrhage in women receiving anticoagulation therapy have been reported (34). The lower platelet count and larger platelets observed in *Larg* KO mice could be due to accelerated new platelet formation in response to low level internal bleeding. To maintain haemostasis, the marrow will release more platelets, and younger platelets are larger in size than older platelets (35). Consistent with this hypothesis, *Larg* KO mice showed a higher percentage of reticulated (young) platelets by thiazole orange staining.

The murine LARG KO utilized in our study is a constitutive KO, and questions may be raised on the specific role of LARG in platelets. Recently, Williams et al. (19) published data from a megakaryocyte and platelet specific *Larg* KO. Consistent with the data presented here, they showed that LARG has an agonist specific role in platelet activation. However there are major differences between the studies. First, we showed that LARG could promote RhoA activation in platelets, a phenomenon not observed in the Williams *et.al* paper. The reasons for the differences could be the duration of agonist treatment, the employment of different panels of agonists and, for the same agonists, different concentrations used between the two studies. These are important, and possibly complementary, distinctions to consider, as RhoA activation is a dose-sensitive, dynamic process. In our study, we used low dose Thrombin (0.01U/ml) to stimulate platelets for 1 min to reveal the differences in RhoA activity. It is possible that when stimulated with different agonists for longer times (e.g. 5 min with 100μM PAR4-AP or 2μM U46), such differences are no longer seen. Furthermore,

in addition to solely checking for RhoA activity, we further examined the phosphorylation of myosin light chain, an important downstream target of RhoA. The reduced MLC phosphorylation further confirmed that RhoA activation is compromised in *Larg* KO platelets. Second, Williams et al reported no difference in platelet count in PF4-Cre mediated *Larg* KO mice suggesting either that the decrease in the *Larg* KO mice reported here are due to deletion of *Larg* from cells other than platelets or that the higher number of mice (n=30 KO mice in our study) assessed in our study was necessary to achieve sensitivity in this assay. In either case, the effect on platelet count is not large. Third, in order to demonstrate the physiological role of LARG in mice, we used two *in vivo* thrombosis models to more convincingly capture both the long-term and acute platelet response to blood vessel damage. Lastly, we also applied a LARG inhibitor to human platelets and showed similar agonist specificity to that observed in *Larg* KO platelets. This underscores the potential clinical and translational value of the findings.

In our *Larg* KO mice, the most significant defects are compromised platelet aggregation and the absence of in vivo thrombus formation, while specific effects on integrin activation and α granule release were milder. We reason that the more pronounced defects overall observed in platelet aggregation and thrombus formation likely result from an accumulation of relatively mild defects that can be assessed in individual steps *in vitro*. The role of LARG in platelet activation is agonist-specific, affecting only thrombin- and thromboxane-induced platelet activation, but not ADP or epinephrine stimulation. It is likely that the agonist specificity is due to LARG transducing signals from only some Gα proteins. Thrombin receptors (PAR-1 and PAR-4 in humans, PAR-3 and PAR-4 in mice) and thromboxane receptors (TPα and TPβ) mainly signal through Gα12/13, but can also activate Gαq at high agonist concentrations (15–17, 37). ADP receptors (P2Y1 and P2Y12) act via both Gαq and Gαi (38), and the epinephrine receptor (α2A-adrenergic receptor) acts via Gαi as well as Gαs (3). In light of the role of LARG in transducing Gα12/13 activation to activate Rho in other cell types (9, 22, 23), it is likely that in platelets, LARG mediates signals from Gα12/13 to downstream activation of RhoA. Because Gα12/13 associates with both thrombin and thromboxane receptors, with deletion of LARG, thrombin and thromboxane induced platelet activation is compromised, while stimulation by ADP or epinephrine remain intact because signals can be transduced through Gαq, Gαi and Gαs. In support of this association, the platelet phenotype of the LARG KO is similar to that reported for Gα13 KO mice (39) and for mice with a megakaryocyte-platelet-specific deletion of RhoA (40). The findings from multiple related studies including PF4-Cre mediated deletion of *Larg* are compared in Supplemental Table 1. All of these KO mice have defective platelet function in response to thrombin and thromboxane, compromised haemostasis and protection from thrombosis. LARG may also act downstream of Gαq (41), and Gαq KO platelets have compromised platelet function (42). However, unlike Gαq KO platelets, *Larg* KO have largely normal platelet function with ADP and collagen stimulation, which were reported to be severely defective in the Gαq KO (42). Therefore, it is less likely that LARG functions downstream of Gαq in platelets. Taken together, the data strongly support a key role for LARG in linking the signaling pathways of Gα13 and RhoA in platelets.

We note that the *Larg* KO phenotype is less severe than that of RhoA KO and the Gα13 KO mice (Supplemental Table 1). This is possibly due to compensatory mechanisms. First is the

potential compensation from other GEF proteins. There are about 70 Dbl-related Rho GEFs expressed in human cells that activate Rho GTPases in specific spatio-temporal contexts (43). Although we have shown that p115-RhoGEF and GEF-H1 are not over-expressed in our KO mice, these two GEFs can function in platelets; *in vitro* assays show that p115-RhoGEF binds thrombin receptors in human platelets (44). Also, GEF-H1 phosphorylation by p21-activated kinases (PAK) is activated downstream of platelet activation by thrombin(45). Another possible compensatory mechanism stems from other Gα signaling subunits, Gαi and Gαs. Platelet activation is an integrated process that requires different G-protein signaling pathways, and signals from two of these pathways can suffice to induce some platelet activation (5, 16). The strain background of the *Larg* KO mice may also explain the mild phenotype. As previously reported, homozygous *Larg* KO on a pure C57Bl6 background is embryonic lethal (9). However, KO mice are viable on a mixed CD1 and C57Bl6 background, with which our study was conducted. In the case of LARG, it is possible that the out-bred background is masking additional defects. Lastly, RhoA has been shown to function downstream of several other platelet receptors (e.g. GPVI receptors and Gαq coupled-receptors) (42, 46) in addition to Gα13, and therefore RhoA KO platelets exhibited moderately reduced aggregate formation upon collagen stimulation (40, 47), defects not observed in our KO model. The LARG inhibitor Y16 sterically blocks binding of LARG to Rho, thereby inhibiting LARG-catalyzed activation of RhoA signaling. This inhibitor also decreases the function of similar RGS RhoGEFs, namely, p115-RhoGEF and PDZ-RhoGEF (18). Studies on the role of the other RGS-RhoGEFs and double, or triple, deletions of these GEFs in platelets can be explored with more severe functional defects expected with double or triple KO.

In summary, we show that LARG is important for human megakaryocyte maturation. LARG also plays an important agonist specific role in platelets through mediating RhoA activation. In addition, the identification of the role of LARG in human platelets implies that inhibiting LARG may be an effective anti-platelet strategy for prevention of pathological thromboses.

Supplementary Material

Refer to Web version on PubMed Central for supplementary material.

Acknowledgments

The authors thank Chad D. Sanada, and Wai Ho (Jack) Tang for helpful discussions, and thank Dr. Silvio J. Gutkind and Dr. Yi Zheng for kindly providing mice and reagents.

Financial support: NIH grants DK094934, DK086267, U54DK106857, and P30 DK0724429.

References

1. Rivera J, Lozano ML, Navarro-Nunez L, et al. Platelet receptors and signaling in the dynamics of thrombus formation. Haematologica. 2009; 94:700–11. [PubMed: 19286885]
2. Cabrera-Vera TM, Vanhauwe J, Thomas TO, et al. Insights into G protein structure, function, and regulation. Endocr Rev. 2003; 24:765–81. [PubMed: 14671004]
3. Li Z, Delaney MK, O'Brien KA, et al. Signaling during platelet adhesion and activation. Arteriosclerosis, thrombosis, and vascular biology. 2010; 30:2341–9.

4. Aittaleb M, Boguth CA, Tesmer JJ. Structure and function of heterotrimeric G protein-regulated Rho guanine nucleotide exchange factors. Molecular pharmacology. 2010; 77:111–25. [PubMed: 19880753]
5. Jin J, Kunapuli SP. Coactivation of two different G protein-coupled receptors is essential for ADP-induced platelet aggregation. Proc Natl Acad Sci U S A. 1998; 95:8070–4. [PubMed: 9653141]
6. Siderovski DP, Willard FS. The GAPs, GEFs, and GDIs of heterotrimeric G-protein alpha subunits. Int J Biol Sci. 2005; 1:51–66. [PubMed: 15951850]
7. Kourlas PJ, Strout MP, Becknell B, et al. Identification of a gene at 11q23 encoding a guanine nucleotide exchange factor: evidence for its fusion with MLL in acute myeloid leukemia. Proc Natl Acad Sci U S A. 2000; 97:2145–50. [PubMed: 10681437]
8. Simon LM, Edelstein LC, Nagalla S, et al. Human platelet microRNA-mRNA networks associated with age and gender revealed by integrated plateletomics. Blood. 2014; 123:e37–45. [PubMed: 24523238]
9. Mikelis CM, Palmby TR, Simaan M, et al. PDZ-RhoGEF and LARG are essential for embryonic development and provide a link between thrombin and LPA receptors and Rho activation. The Journal of biological chemistry. 2013; 288:12232–43. [PubMed: 23467409]
10. Brass LF. Thrombin and platelet activation. Chest. 2003; 124:18S–25S. [PubMed: 12970120]
11. Pronk CJ, Rossi DJ, Mansson R, et al. Elucidation of the phenotypic, functional, and molecular topography of a myeloerythroid progenitor cell hierarchy. Cell Stem Cell. 2007; 1:428–42. [PubMed: 18371379]
12. Godin D, Ivan E, Johnson C, et al. Remodeling of Carotid Artery Is Associated With Increased Expression of Matrix Metalloproteinases in Mouse Blood Flow Cessation Model Circulation. 2000; 102:2861–6. [PubMed: 11104745]
13. Tang WH, Stitham J, Jin Y, et al. Aldose reductase-mediated phosphorylation of p53 leads to mitochondrial dysfunction and damage in diabetic platelets. Circulation. 2014; 129:1598–609. [PubMed: 24474649]
14. Owens AP 3rd, Lu Y, Whinna HC, et al. Towards a standardization of the murine ferric chloride-induced carotid arterial thrombosis model. J Thromb Haemost. 2011; 9:1862–3. [PubMed: 21884567]
15. Moers A, Wettschureck N, Gruner S, et al. Unresponsiveness of platelets lacking both Galpha(q) and Galpha(13). Implications for collagen-induced platelet activation. The Journal of biological chemistry. 2004; 279:45354–9. [PubMed: 15326177]
16. Nieswandt B, Schulte V, Zywietz A, et al. Costimulation of Gi- and G12/G13-mediated signaling pathways induces integrin alpha IIbbeta 3 activation in platelets. The Journal of biological chemistry. 2002; 277:39493–8. [PubMed: 12183468]
17. Coughlin SR. Protease-activated receptors in hemostasis, thrombosis and vascular biology. Journal of Thrombosis and Haemostasis. 2005; 3:1800–14. [PubMed: 16102047]
18. Shang X, Marchioni F, Evelyn CR, et al. Small-molecule inhibitors targeting G-protein-coupled Rho guanine nucleotide exchange factors. Proc Natl Acad Sci U S A. 2013; 110:3155–60. [PubMed: 23382194]
19. Williams CM, Harper MT, Goggs R, et al. Leukemia-associated Rho guanine-nucleotide exchange factor is not critical for RhoA regulation, yet is important for platelet activation and thrombosis in mice. J Thromb Haemost. 2015
20. Stojanovic A, Marjanovic JA, Brovkovych VM, et al. A phosphoinositide 3-kinase-AKT-nitric oxide-cGMP signaling pathway in stimulating platelet secretion and aggregation. The Journal of biological chemistry. 2006; 281:16333–9. [PubMed: 16613861]
21. Woulfe D, Jiang H, Morgans A, et al. Defects in secretion, aggregation, and thrombus formation in platelets from mice lacking Akt2. The Journal of clinical investigation. 2004; 113:441–50. [PubMed: 14755341]
22. Medlin MD, Staus DP, Dubash AD, et al. Sphingosine 1-phosphate receptor 2 signals through leukemia-associated RhoGEF (LARG), to promote smooth muscle cell differentiation. Arteriosclerosis, thrombosis, and vascular biology. 2010; 30:1779–86.
23. Ying Z, Jin L, Palmer T, et al. Angiotensin II up-regulates the leukemia-associated Rho guanine nucleotide exchange factor (RhoGEF), a regulator of G protein signaling domain-containing

RhoGEF, in vascular smooth muscle cells. Molecular pharmacology. 2006; 69:932–40. [PubMed: 16354763]

24. Kiel MJ, Yilmaz OH, Iwashita T, et al. SLAM family receptors distinguish hematopoietic stem and progenitor cells and reveal endothelial niches for stem cells. Cell. 2005; 121:1109–21. [PubMed: 15989959]
25. Osawa M, Hanada K, Hamada H, et al. Long-term lymphohematopoietic reconstitution by a single CD34-low/negative hematopoietic stem cell. Science. 1996; 273:242–5. [PubMed: 8662508]
26. Sitnicka E, Buza-Vidas N, Larsson S, et al. Human CD34+ hematopoietic stem cells capable of multilineage engrafting NOD/SCID mice express flt3: distinct flt3 and c-kit expression and response patterns on mouse and candidate human hematopoietic stem cells. Blood. 2003; 102:881–6. [PubMed: 12676789]
27. Larochelle A, Savona M, Wiggins M, et al. Human and rhesus macaque hematopoietic stem cells cannot be purified based only on SLAM family markers. Blood. 2011; 117:1550–4. [PubMed: 21163926]
28. Antonchuk J, Sauvageau G, Humphries RK. HOXB4-induced expansion of adult hematopoietic stem cells ex vivo. Cell. 2002; 109:39–45. [PubMed: 11955445]
29. Amsellem S, Pflumio F, Bardinet D, et al. Ex vivo expansion of human hematopoietic stem cells by direct delivery of the HOXB4 homeoprotein. Nat Med. 2003; 9:1423–7. [PubMed: 14578882]
30. Wang L, Menendez P, Shojaei F, et al. Generation of hematopoietic repopulating cells from human embryonic stem cells independent of ectopic HOXB4 expression. J Exp Med. 2005; 201:1603–14. [PubMed: 15883170]
31. Iwasaki H, Akashi K. Hematopoietic developmental pathways: on cellular basis. Oncogene. 2007; 26:6687–96. [PubMed: 17934478]
32. Parekh C, Crooks GM. Critical differences in hematopoiesis and lymphoid development between humans and mice. J Clin Immunol. 2013; 33:711–5. [PubMed: 23274800]
33. Terzic M, Likic I, Pilic I, et al. Conservative management of massive hematoperitoneum caused by ovulation in a patient with severe form of von Willebrand disease--a case report. Clinical and experimental obstetrics & gynecology. 2012; 39:537–40. [PubMed: 23444764]
34. Gupta A, Gupta S, Manaktala U, et al. Conservative management of corpus luteum haemorrhage in patients on anticoagulation: a report of three cases and review of literature. Archives of gynecology and obstetrics. 2015; 291:427–31. [PubMed: 25106126]
35. Guthikonda S, Alviar CL, Vaduganathan M, et al. Role of reticulated platelets and platelet size heterogeneity on platelet activity after dual antiplatelet therapy with aspirin and clopidogrel in patients with stable coronary artery disease. Journal of the American College of Cardiology. 2008; 52:743–9. [PubMed: 18718422]
36. Chiu WC, Juang JM, Chang SN, et al. Angiotensin II regulates the LARG/RhoA/MYPT1 axis in rat vascular smooth muscle in vitro. Acta pharmacologica. Sinica. 2012; 33:1502–10.
37. Booden MA, Siderovski DP, Der CJ. Leukemia-associated Rho guanine nucleotide exchange factor promotes G alpha q-coupled activation of RhoA. Mol Cell Biol. 2002; 22:4053–61. [PubMed: 12024019]
38. Gachet C. P2 receptors, platelet function and pharmacological implications. Thrombosis and haemostasis. 2008; 99:466–72. [PubMed: 18327393]
39. Moers A, Nieswandt B, Massberg S, et al. G13 is an essential mediator of platelet activation in hemostasis and thrombosis. Nat Med. 2003; 9:1418–22. [PubMed: 14528298]
40. Pleines I, Hagedorn I, Gupta S, et al. Megakaryocyte-specific RhoA deficiency causes macrothrombocytopenia and defective platelet activation in hemostasis and thrombosis. Blood. 2012; 119:1054–63. [PubMed: 22045984]
41. Pfreimer M, Vatter P, Langer T, et al. LARG links histamine-H1-receptor-activated Gq to Rho-GTPase-dependent signaling pathways. Cellular signalling. 2012; 24:652–63. [PubMed: 22100544]
42. Offermanns S, Toombs CF, Hu YH, et al. Defective platelet activation in G alpha(q)-deficient mice. Nature. 1997; 389:183–6. [PubMed: 9296496]
43. Rossman KL, Der CJ, Sondek J. GEF means go: turning on RHO GTPases with guanine nucleotide-exchange factors. Nat Rev Mol Cell Biol. 2005; 6:167–80. [PubMed: 15688002]

44. Huang JS, Dong L, Kozasa T, et al. Signaling through G(alpha)13 switch region I is essential for protease-activated receptor 1-mediated human platelet shape change, aggregation, and secretion. The Journal of biological chemistry. 2007; 282:10210–22. [PubMed: 17298951]

45. Aslan JE, Baker SM, Loren CP, et al. The PAK system links Rho GTPase signaling to thrombin-mediated platelet activation. American journal of physiology Cell physiology. 2013; 305:C519–28. [PubMed: 23784547]

46. Jin J, Mao Y, Thomas D, et al. RhoA downstream of G(q) and G(12/13) pathways regulates protease-activated receptor-mediated dense granule release in platelets. Biochemical pharmacology. 2009; 77:835–44. [PubMed: 19073150]

47. Goggs R, Williams CM, Mellor H, et al. Platelet Rho GTPases-a focus on novel players, roles and relationships. The Biochemical journal. 2015; 466:431–42. [PubMed: 25748676]

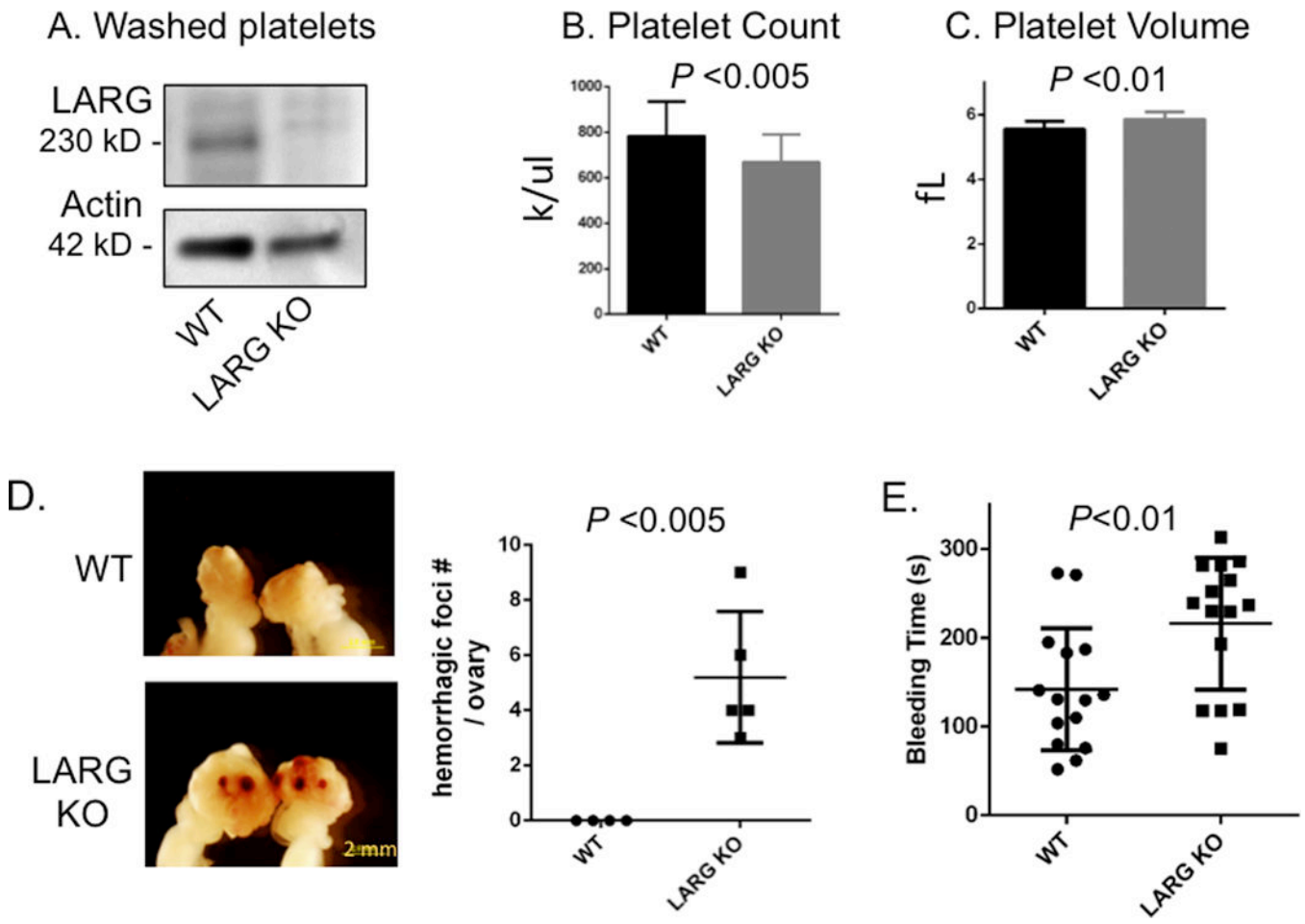

Figure 1. Platelet changes in LARG KO mice and defective hemostasis

(A) Analysis of LARG protein expression in WT and LARG KO platelets. Actin was used as loading control. (B,C) Peripheral platelet count (B) and platelet volume (C) of WT and LARG KO littermates. Data are presented as mean + SD of 10-30 mice per group. fL indicates femtoliter. (D) Representative images of gross appearance of ovaries of 8-week-old WT and LARG KO littermates with number of hemorrhagic foci/ovary quantified in graph (WT n=4; LARG KO n=5) (E) Tail bleeding times of WT and LARG KO littermates. Each symbol represents 1 mouse (n=15/genotype).

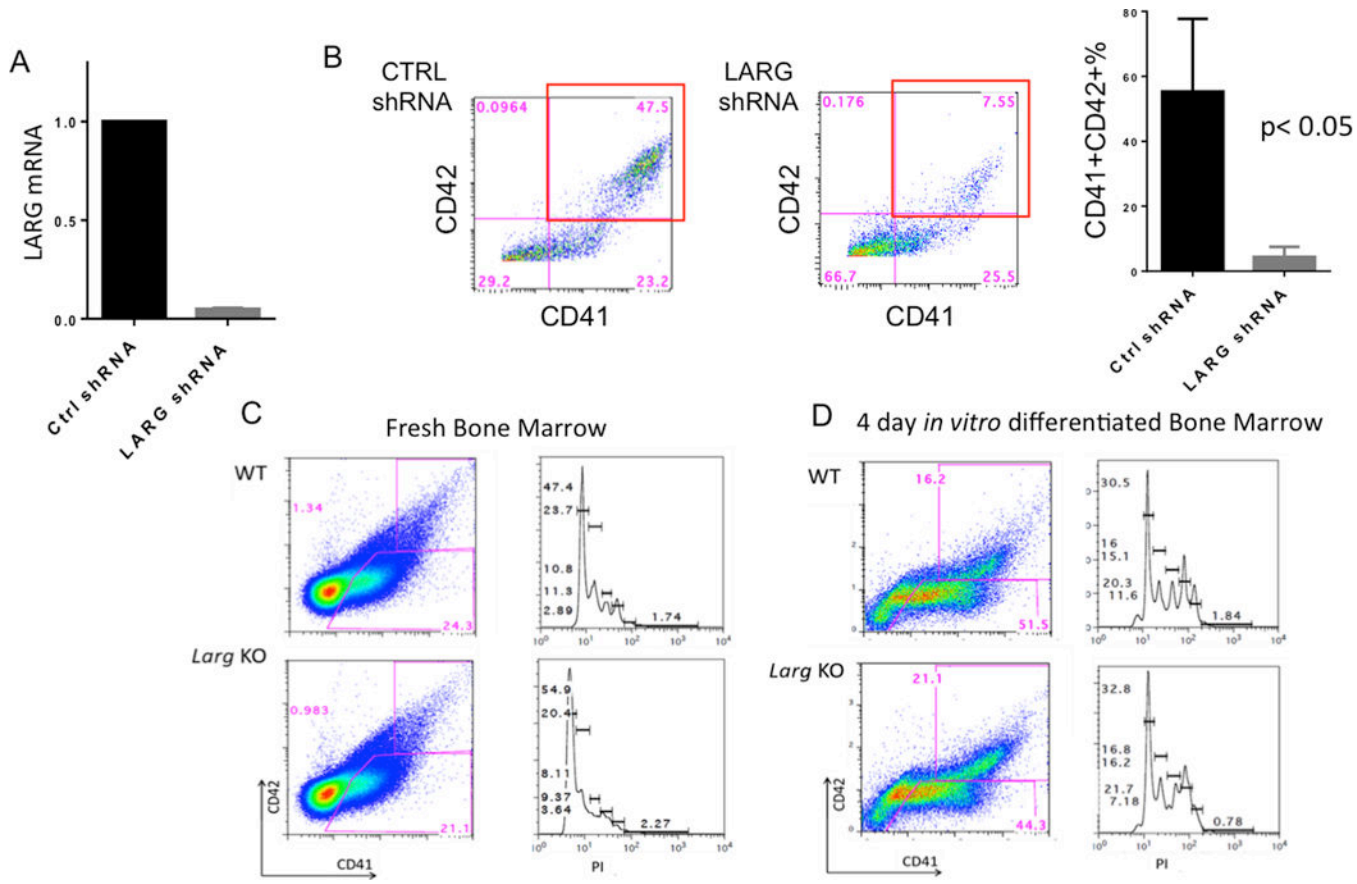

Figure 2. LARG plays a role in human, but not murine, megakaryocyte maturation

(A) qRT-PCR on puromycin selected control or LARG shRNA (shRNA-1 used) knockdown in primary human MEP differentiated in vitro confirmed an over 80% knockdown of LARG. (B) Flow cytometric analysis for CD41 and CD42 expression shows a block in MK differentiation with LARG KD. Right bar plot is mean + SD of three independent experiments ($p<0.05$). (C-D) Flow cytometric analysis for CD41 and CD42 (left) and ploidy of gated CD41+ cells (right) in fresh (C) and in vitro differentiated (D) murine bone marrow cells shows no difference in megakaryocyte number, percentage, cell surface markers or ploidy in WT versus *Larg* KO. Representative data are shown (n=3 per genotype).

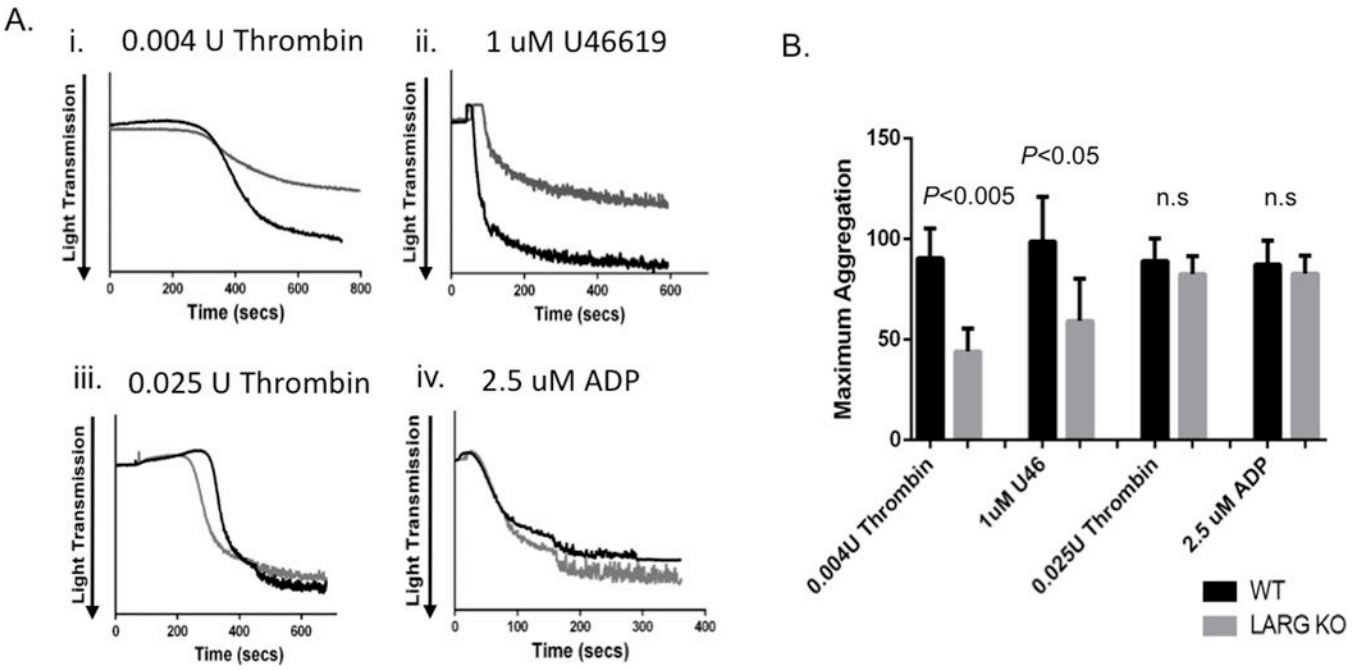

Figure 3. Reduced aggregation in *Larg* KO platelets by thrombin and thromboxane stimulation

(A) Washed platelets were stimulated with the indicated agonists, and light transmission was recorded on a Chronolog aggregometer. Representative platelet aggregation traces are shown. (B) Graph of mean and SD of the maximal aggregation from four independent experiments (n= 4/genotype); Max aggregation of 100% would be equivalent to light transmission through media control without platelet addition.

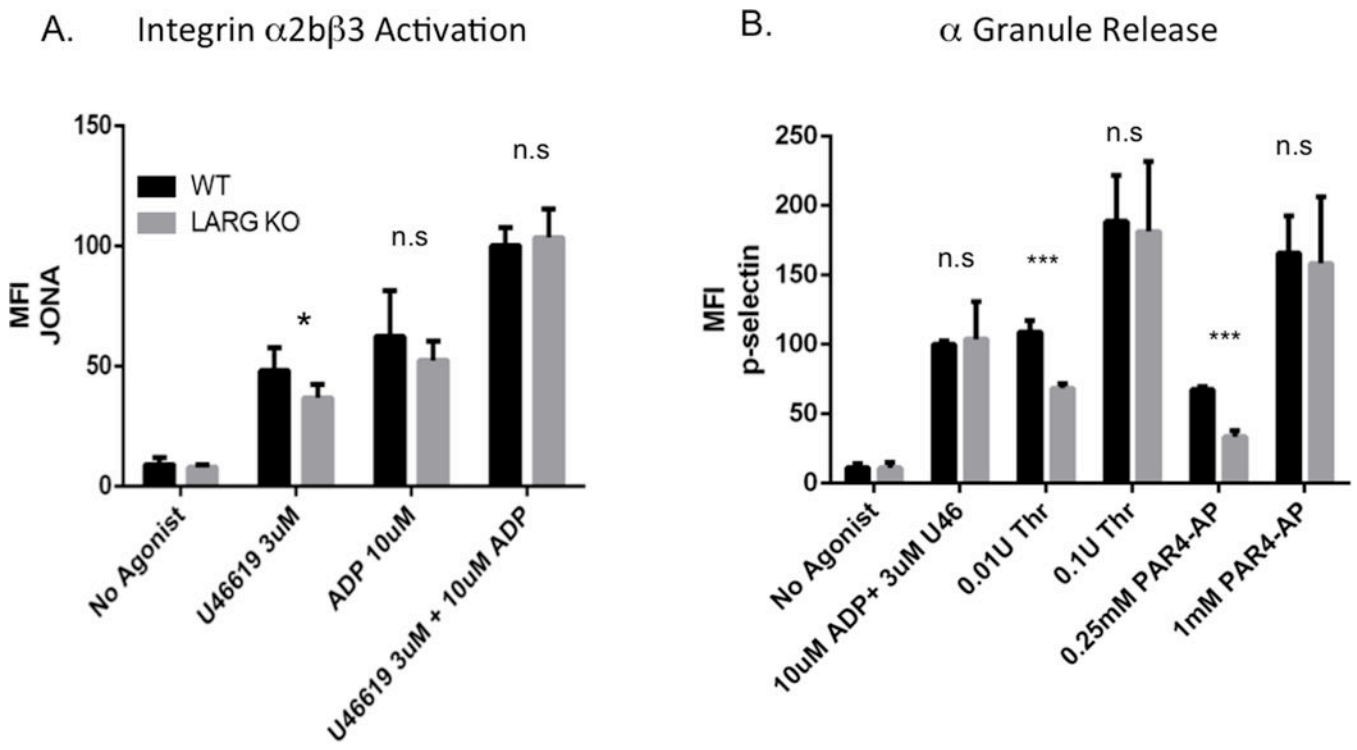

Figure 4. ***Larg*** **KO platelets have agonist-specific impaired integrin activation and α granule release**

Flow cytometric analysis of integrin α2bβ3 activation (binding of JONA antibody) (A) and degranulation-dependent P-selectin exposure (B) in response to the indicated agonists in WT and *Larg* KO platelets. Data are mean fluorescence intensities (MFI) and SD of 6-8 mice per genotype from a combination of 3 independent experiments. (*P<0.05;***P<0.001)

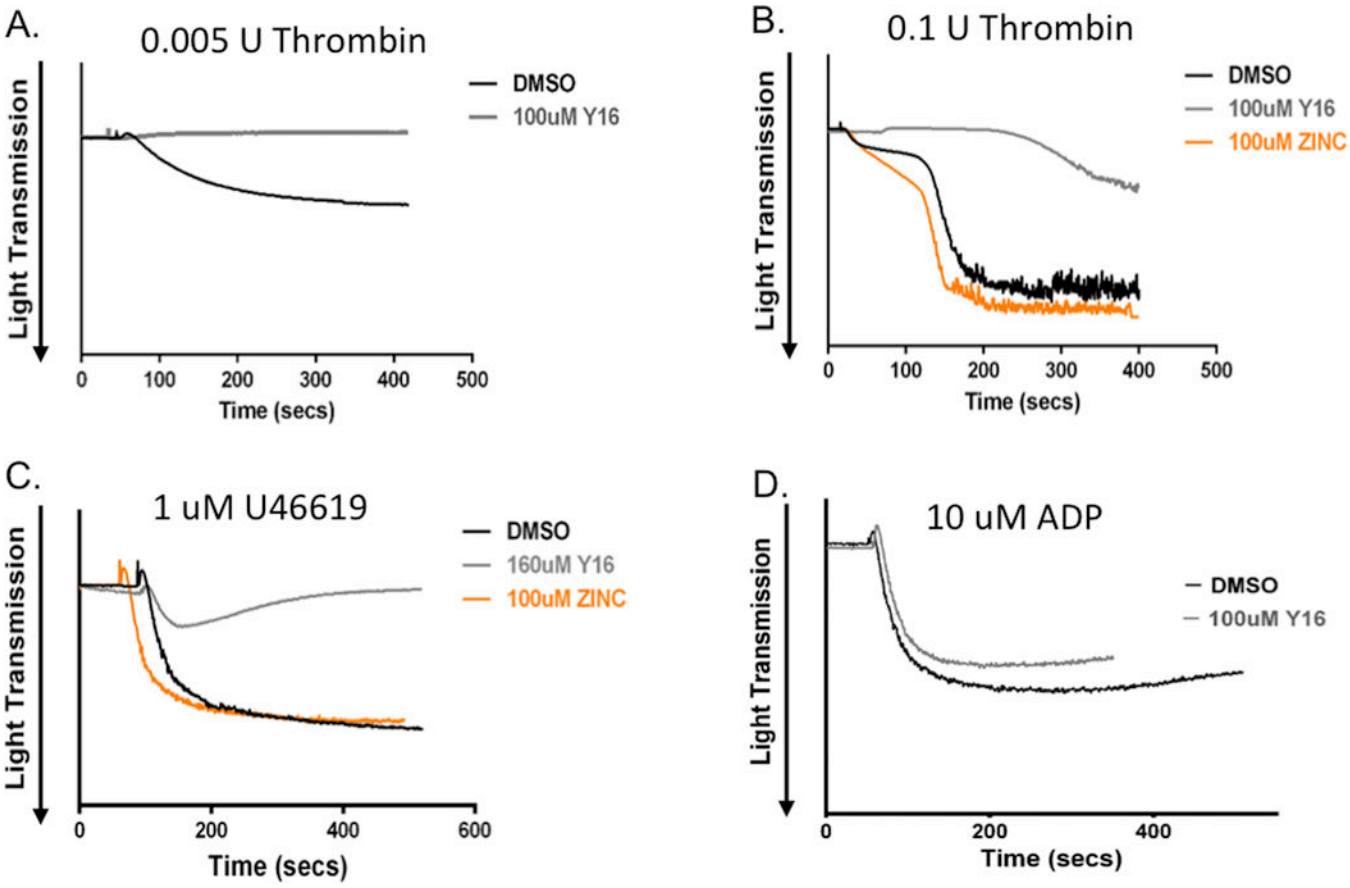

Figure 5. Y16 inhibits thrombin and thromboxane induced human platelet aggregation

(A-D) Human washed platelets were incubated with DMSO, LARG inhibitor Y16 or negative control compound ZINC, as indicated, before adding indicated agonists. Representative data from 3 individual experiments from 3-4 different donors.

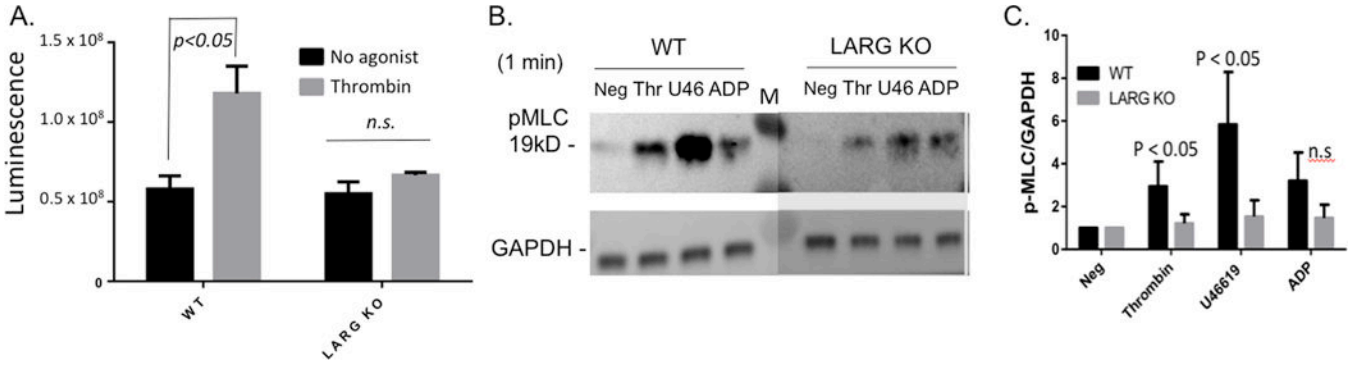

Figure 6. *Larg* KO platelets have compromised RhoA activation and myosin light chain phosphorylation upon thrombin and thromboxane stimulation

(A) Detection of activated RhoA by G-LISA luminescence assay in washed platelets before (black) and after (gray) 1 min 0.01U/ml thrombin. Raw luminescence is shown. No difference is observed in basal (no agonist) RhoA activity between WT and *Larg* KO. (B) Detection of myosin light chain phosphorylation in platelet lysates after stimulation with different agonists. (Neg=No agonist; Thr=0.01U/ml thrombin; U46=1uM U46619; ADP (5uM); M=molecular weight marker). Image from one blot is shown with *Larg* part darkened to equalize GAPDH for ease of view. This does not affect quantitation shown in C. (C) Relative amount of phosphorylated (P)-MLC normalized to GAPDH for each experiment. Data for 4 separate experiments are graphed with the P-MLC level at baseline normalized to 1 for each experiment.

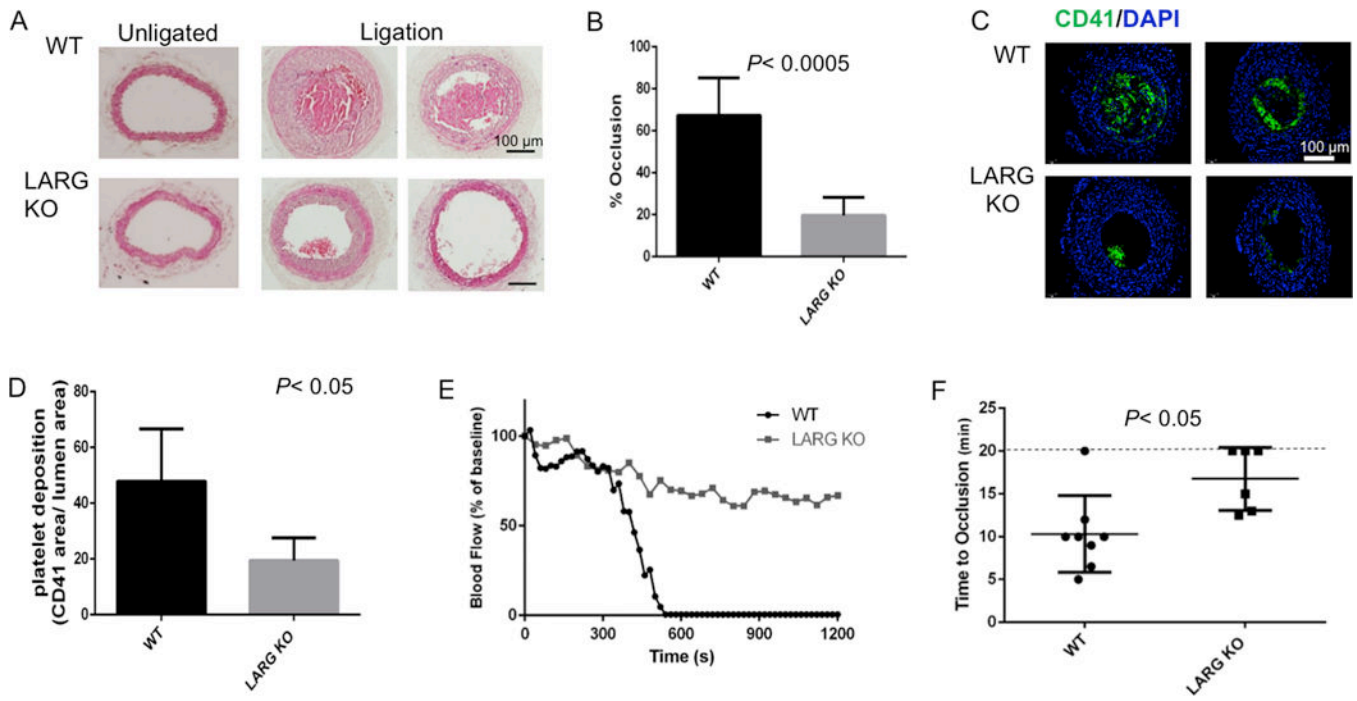

Figure 7. *Larg* KO mice are protected from thrombus formation in carotid artery injury models

(A) Representative images (8 mice/genotype, 2 independent experiments) of H&E staining of cross sections from un-ligated and ligated carotid arteries from WT and *Larg* KO mice. (B) Percentage occlusion was calculated by dividing the area of thrombus by the vessel lumen area. (C) Platelet deposition was assessed by immunofluorescence for CD41 and (D) quantified by dividing CD41+ area by lumen area. (E) Representative time-course of carotid arterial blood flow following FeCl3 application outside the arterial wall of WT and *Larg* KO mice. (F) Statistical analysis of time to occlusion of 3 independent experiments. Each symbol represents 1 mouse (WT n=8; KO n=6).